MORPHOLOGY AND CATHODE OPTIMIZATION FOR EFFICIENT POLYMER BULK HETEROJUNCTION SOLAR CELLS

by

YI YANG

Presented to the Faculty of the Graduate School of
The University of Texas at Arlington in Partial Fulfillment
of the Requirements
for the Degree of

MASTER OF SCIENCE IN MATERIALS SCIENCE AND ENGINEERING

THE UNIVERSITY OF TEXAS AT ARLINGTON

May 2009

ACKNOWLEDGEMENTS

I sincerely thank Dr. Choong-Un Kim for his support and for being my committee member. I would also like to thank Dr. Dong-Chan Shin for reviewing my thesis work and for being my committee member. I express my gratitude to all the professors and the department staff for offering their support whenever required, especially our secretary, Jennifer Standlee for helping me with ordering research supplies and with my academic paperwork.

I would like to say thanks to Dr. Dong-Chan Shin, who gave many valuable suggestions with his rich experience and knowledge. I appreciate the help of Mr. Eduardo Maldonado at Nanofab who trained me on various equipments. I also would like to thank Dr. Jiechao Jiang for his support in using the characterization equipments at Characterization Center for Materials and Biology. I also thank NASA Glenn Research Center for their support in cell characterization.

I appreciate the help of my colleagues and all the friends who motivated and supported me during my thesis work. I express my thanks to Xin Wang, who introduced me to Jin's group and showed me the world of solar cell. I thank Chun-Young Lee who taught me cell fabrication during my first semester in this group. I thank Dr. Ki-Hyun Kim, Alex Alphonse, Houkuan Lee, Shenbin Wu, Ammena, Soo Kim, Xiaofei Han, Chienwen Huang, Jie He, Beibei Wang and Jingwen He for their consistent support during my entire graduate career.

Finally I devote my heartiest appreciation to my parents and my grandmother for their love and affection that inspired me throughout my life.

April 14, 2009

ABSTRACT

MORPHOLOGY AND CATHODE OPTIMIZATION FOR
EFFICIENT POLYMER BULK HETEROJUNCTION
SOLAR CELLS

Yi Yang, M.S.

The University of Texas at Arlington, 2009

Supervising Professor: Michael Jin

Efficiency of polymer bulk heterojunction solar cell is highly dependent on the active layer morphology and can be controlled by specific experimental conditions. In this work, the influences of P3HT:PCBM blend composition, solution concentration, and the thermal annealing on the cell performance are presented. The maximum of J_{sc} and FF are reached when the weight percentage of PCBM in the blend is 60 % under which both high density of donor and accepter interfaces expecting the formation of efficient percolated electron transport paths. 36 mg/ml is found to be the optimum solution concentration for P3HT:PCBM blend and it can be explained by the relationship between the active layer thickness and resistance. Finally, it is observed that the J_{sc} and V_{oc} increase from 2.04 mA and 0.47 V to 10.65 mA and 0.58 V respectively after the devices are annealed at 150 ℃ for 20 min. The increase in J_{sc}, in particular, can be attributed to the donor/accepter phase separation and charge carrier mobility increase caused by P3HT crystallization. The light absorption increase in active layer by annealing is also responsible for the J_{sc} increases.

In order to increase the FF, charge accumulation expected at the Al/PCBM interface is prevented by depositing Ca prior to Al, which produces higher electrical field at the interface due

to the lower work function of Ca compared to Al. The increased electrical field can eliminate the charge barrier at the interface and facilitate the transport of electrons from PCBM to the cathode. In this work, cells with Al and Ca/Al bilayer as the cathodes are fabricated respectively to study the effect of Ca on the cell performance. Compared to cells with Al cathode, FF of the cells with Ca/Al cathode has increased from 21% to 51%. Also, both J_{sc} and V_{oc} of the cells increase from 9.81 mA/cm^2 to 11.22 mA/cm^2 and 0.53 V to 0.65 V, respectively. The highest efficiency of 3.32% is realized.

TABLE OF CONTENTS

LIST OF ILLUSTRATIONS

LIST OF TABLES

OVERVIEW

The thesis has been divided into two major chapters because the polymer bulk heterojunction solar cell is investigated from two different aspects:

1. Chapter 1 – Optimization of morphology for organic solar cell
2. Chapter 2 – Realization of efficient organic solar cell with calcium/aluminum cathode

In Chapter 1, by control of the composition and the solution concentration of a blend made of electron-donating and electron-accepting organic molecules, the morphology of organic absorber in polymer solar cell is optimized and their effects on efficiency have been studied. Also, annealing is carried out to optimize donor/accepter phase separation and its influences on the performance of polymer solar cell are studied.

In Chapter 2, Ca/Al bilayer cathode is employed to improve the charge collection in polymer solar cell. As a result, and the power conversion efficiency over 3% is realized. Mechanisms of the improvement have been studied.

CHAPTER 1

OPTIMIZATION OF MORPHOLOGY FOR ORGANIC SOLAR CELL

1.1 Introduction

The high cost of traditional photovoltaic devices has prohibited the technology from having a significant impact on global energy production. However, photovoltaics (PV) is still of continued high interest because of the fact that they represent the only truly portable renewable-energy conversion technology available today. The expensive investment in costly semiconductor processing technologies is the essential limit for the production of photovoltaic cells. Therefore, photovoltaic devices fabricated on thin plastic substrate and manufactured by techniques such as reel-to-reel printing is highly attractive with regard to cost. In order to realize this idea, technologies for large-area coating must be applied to a low-cost material class. These requirements can be fulfilled by solution processable organic and inorganic semiconductors. Flexible chemical tailoring allows the design of organic semiconductors with the desired properties, and printing or coating techniques like screen-printing, inkjet, offset, and flexography are being established for semiconducting polymers today, driven by display and general electronic device demands.

Generally, organic photovoltaics (OPV) have many attractive features, among them: (a) the potential to be flexible and semitransparent, (b) the possibility to be manufactured in a continuous printing process, (c) fabrication by means of large-area coating, (d) convenient integration in a wide variety of devices, (e) greatly reduced costs compared with traditional photovoltaics, and (f) significant ecological and economic advantages [1].

1.1.1 Solar Cell and Its Characteristics

Photovoltaics is the field of technology and research related to the application of solar cells for energy by converting sunlight directly into electricity. Due to the growing demand for

clean sources of energy, the manufacture of solar cells has expanded dramatically in recent years [2].

The most important figures of merit describing the performance of a solar cell are the open circuit voltage (V_{oc}), the short circuit current (J_{sc}), the fill factor (FF) and the power conversion efficiency (PCE). Typical current versus voltage curves under dark and illumination are shown in Figure 1.1. The FF is given by the quotient of maximum power (yellow rectangle in the figure) and the product of open circuit voltage and short circuit current (white rectangle). The efficiency is the ratio of maximum power to incident radiant power.

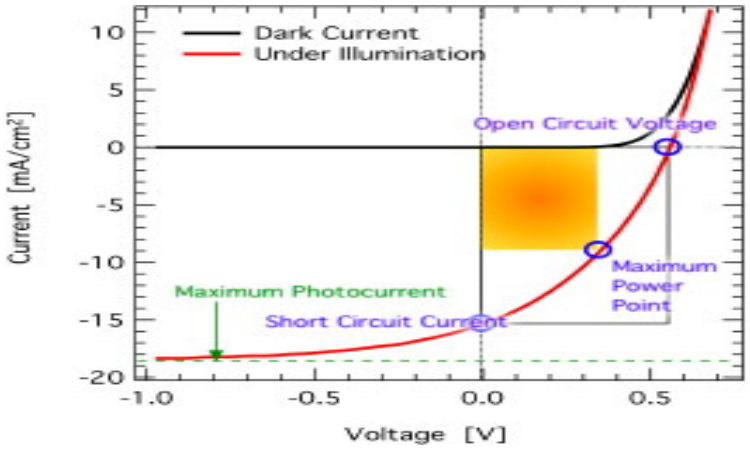

Figure 1.1: I-V curve of a typical solar cell [3].

1.1.2 Organic Photovoltaic Device

A photovoltaic device which incorporates organic molecules is called organic photovoltaic device. In organic photovoltaic devices, the primary effect upon exposure to solar light is a photoinduced electron transfer between donor- and acceptor-type semiconducting polymers or molecules, yielding a charge-separated state. This photoinduced electron transfer between donor and acceptor boosts the photogeneration of free charge carriers, as compared with the individual, pure materials, in which the formation of bound electron–hole pairs, or excitons, is generally favored. In combining electron-donating and electron-accepting materials in the active layer of a solar cell, excitons created in either material can diffuse to the donor/acceptor interface, i.e. between materials with sufficiently different highest occupied

molecular orbital (HOMO) and lowest unoccupied molecular orbital (LUMO) respectively. The material with larger LUMO will act as electron acceptor (A) and the one with smaller LUMO value will act as electron donor (D). To achieve efficient charge separation we need:

$$\Delta (LUMO_D\text{-}LUMO_A) > \text{Exciton energy [4].}$$

1.1.3 Organic Bulk Heterojunction Solar Cell

Due to their short lifetime and low mobility, the diffusion length of excitons in organic semiconductors is limited to about 10 nm only [5]. This imposes an important condition on efficient charge separation. Anywhere in the active layer, the distance to the interface should be on the order of the exciton diffusion length. Despite their high absorption coefficients, exceeding 10^5 cm^{-1}, a 20 nm double layer of donor and acceptor materials would not be optically dense, allowing most photons to pass freely. The solution to this dilemma is elegantly simple [6, 7]. By simply mixing the donor and accepter materials randomly and relying on the intrinsic tendency of polymer materials to phase-separate on a nanometer dimension, junctions throughout the bulk of the material are created that ensure quantitative dissociation of photogenerated excitons, irrespective of the thickness.

Polymer–fullerene solar cells were among the first to utilize this bulk heterojunction principle [6]. However, this attractive solution poses a new challenge. Photogenerated charges must be able to migrate to the collecting electrodes through this intimately mixed blend. Because holes are transported by the donor material and electrons by the accepter material, these materials should be preferably mixed into a bicontinuous, interpenetrating network in which inclusions or barrier layers are avoided. The close-to-ideal bulk heterojunction solar cell may look like the illustration in Figure 1.2.

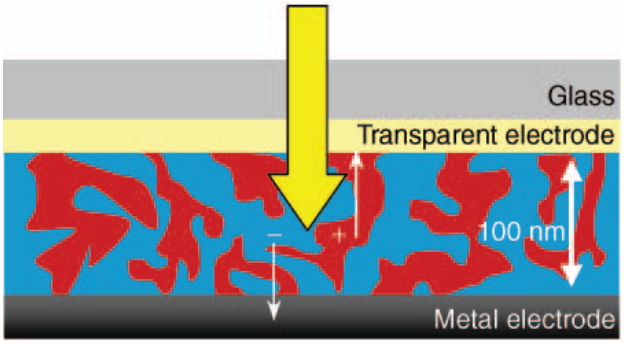

Figure 1.2: Schematic representation of a bulk heterojunction solar cell, showing the phase separation between donor (red) and acceptor (blue) materials [5].

The basic structure of the solar cell is shown in the Figure 1.3. It consists of indium tin oxide (ITO) coated glass as the bottom anode over which the hole transport layer, poly(3,4-ethylenedioxythiophen): polystyrene sulfonic acid (PEDOT:PSS) is formed. An active layer, a blend of poly(3-hexylthiophene) (P3HT) and 1-(3-methoxycarbonyl)propyl-1-phenyl[6,6]C61 (PCBM) is spin coated on top of PEDOT:PSS to absorb the light. Finally the top metal cathode is deposited.

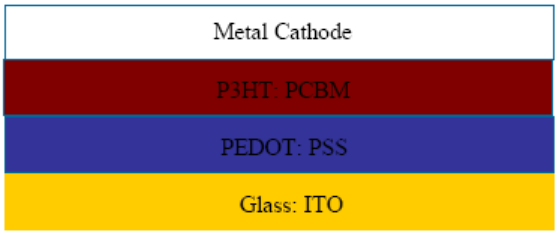

Figure 1.3: Typical structure of a polymer bulk heterojunction solar cell.

Devices with the bulk heterojunction structure using conjugated polymers and fullerenes have shown the highest efficiencies compared to other types of organic solar cells, such as organic small molecule solar cells and dye-sensitized solar cell. PCE of about 5% was achieved based on P3HT and PCBM as the donor and acceptor respectively [8, 9, 10].

1.1.4 Morphology of Polymer/Fullerene Bulk Heterojunction Solar Cell

Organic photovoltaic device is highly dependent on the nanoscale morphology of the two components (donor/acceptor) in the photoactive layer. In order to achieve high efficiency solar cells, the nanometer morphology of the bulk heterojunctions should facilitate both the photo induced creation of mobile charge carriers (the optimum density of donor/acceptor interfacial contact) as well as transport of the carriers. Also the charge carrier mobility is highly dependent on the morphology and higher crystallization of the photoactive polymer-fullerene blend is preferred. The morphology can be affected by controlling several experimental parameters during the film formation or by treatments afterwards. Experimentally the following parameters have been identified as most significant for their influence on the nanoscale morphology in these polymer–fullerene blends [11]:

a) spin coating solvent,

b) composition between polymer and fullerene,

c) solution concentration,

d) controlled phase separation and crystallization induced by thermal annealing, and finally

e) the chemical structure of the materials.

For instance, using the blend of poly[2-methoxy-5-(2'-ethyl-hexyloxy)-1,4-phenylene vinylene] (MEH-PPV) and PCBM as the active layer, Shaheen *et al.* observed a strong dependence of the performance on the solvent used; whereas toluene cast devices yielded power conversion efficiencies of only 0.9%, the use of chlorobenzene almost tripled the efficiency [10]. Also in the study of blending ratio, Gao *et al.* discussed the solar cell device parameters J_{sc} and V_{oc} of MEH-PPV:C_{60} bulk heterojunctions in terms of their dependence on the C_{60} content [12]. Although the V_{oc} dropped upon the addition of only small amounts of C_{60} to MEH-PPV, the photocurrent and also the power conversion efficiency were still increasing up to the largest C_{60} content of 80%. To investigate the influence of the solution concentration, H. Hoppe *et al.* prepared solutions of different concentrations but with constant mixing ratio

between MDMO-PPV and PCBM (1: 4 by weight) [11]. It was confirmed that the average film thickness and the fullerene cluster size are increased with higher concentration, which can determine the light absorption and series resistance of the active layer, charge carrier generation, and donor/accepter phase separation in the active layer respectively. Padinger *et al.* reported recently on postproduction treatments of P3HT:PCBM bulk heterojunction solar cells [13]. After a combined heat and applied DC voltage postproduction treatment, the power conversion efficiency could be raised to 3.5% from the improved active layer morphology and the removal of shunts respectively.

In this study, effects of the composition between P3HT:PCBM and the solution concentration of active layer on cell performance are studied. Also thermal annealing is carried out at different conditions to learn its effect on the polymer solar cell performance.

1.2 Experimental Setup

In this section, the materials and device fabrication procedures for P3HT:PCBM bulk heterojunction solar cells have been given. Also, the various characterization techniques used are provided.

1.2.1 Materials and Device Fabrication

ITO is chosen as an anode in this study due to its high transparency and low resistivity. ITO coated glass sheets are purchased from Sigma Aldrich and its resistivity is 15-25 ohm/sq. Before cleaning, ITO substrates masked with Scapa tapes are put into 32 vol% hydrochloric acid (HCl) for 30 min for patterning. Then, the patterned ITO substrates are cleaned in an ultrasonic bath using soap water, toluene, acetone and isopropanol sequentially for 20 min respectively.

After the cleaning of ITO substrates, PEDOT:PSS is spin coated on top of the ITO coated glass at 5000 rpm for 30 sec producing thickness of 20-40nm. It is annealed at 80 ℃ for 10 min to drive off solvent (water) molecules. Both spin coating and annealing are carried out in the ambient air. PEDOT: PSS in this study is obtained from H.C. Starck Inc. PEDOT:PSS

(Figure1.4) is widely used for OPV and organic light emitting diode (OLED) devices because its highest occupied molecular orbital (HOMO) value is as high as 5.2eV [14] so that it can work as a hole transport layer. It has a high electrical conductivity in the range of 400-600 S/cm and high optical transparency [15]. What is more, it is stable in the oxidized state and can meet the requirement of outdoor applications.

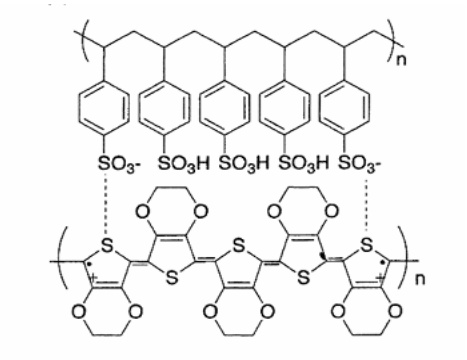

Figure 1.4: Structure of Poly (3, 4-ethylenedioxythiophen)/polystyrene sulfonic acid [16].

For the fabrication of polymer bulk heterojunction, a chlorobenzene solution of regioregular P3HT and PCBM is prepared and spin-coated to deposit a P3HT:PCBM absorber layer on top of the PEDOT:PSS. P3HT and PCBM are purchased respectively from Sigma Aldrich and Solenne B.V. and used as received without further purification. The chlorobenzene is chosen because higher cell efficiency is obtained from it compared to other solvents, such as chloroform and dichlorobenzene [19]. The solutions are spin-coated at 1500 rpm for 30 sec and repeated once to increase the thickness of the active layer. Then the samples are baked on the hot plate at different temperatures for 20 min respectively to study its effect on cell performance. The all processes associated with the P3HT:PCBM layer are performed under the ambient air.

Polythiophene belongs to a class of polymers made up of alternate single and double C-C bond and is an example for π-conjugated systems. It is of increasing interest because of the combination of electronic properties, environmental stability and their structural properties. Environmental stability allows the device fabrication in ambient air, yet resulting in working solar

cells as demonstrated in this study. Polythiophene is made soluble in organic solvents by the alkyl substitution of the thiophene ring and the solubility increases with increasing the chain length of the substitute. P3HT (Figure 1.5) is one of the polythiophene derivatives and widely used as electron donor because of its low band gap and high hole mobility.

Buckminster fullerene (C_{60}) is widely used as electron acceptor because of its high electron mobility. The solubility of the pristine C_{60} is limited in many solvents and hence it is structurally modified to PCBM (Figure 1.6), which shows practical solubility in many organic solvents like chloroform, chlorobenzene, etc.

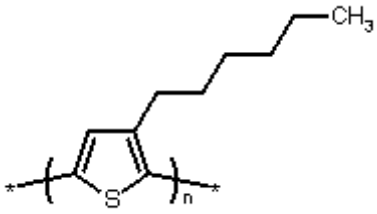

Figure 1.5: Structure of poly(3-hexylthiophene-2,5-diyl) [17].

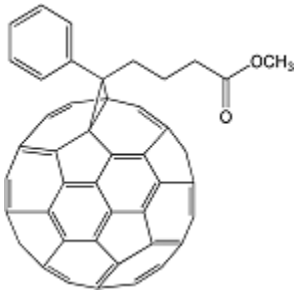

Figure 1.6: Structure of (6,6)-phenyl C_{61} butyric acid methyl ester [18].

In this work, firstly, various batches of devices are made with varying PCBM content to study the effect of the composition between P3HT and PCBM on cell performance. Secondly, P3HT:PCBM blends with the same PCBM content are dissolved in different amounts of chlorobenzene to learn the cell performance dependence on solution concentration. Thirdly, after the active layer is spin-coated, devices are annealed at different temperatures to check

thermal annealing influence on cell performance. Also, the optical transmittances of P3HT:PCBM layers directly spin-coated on quartz substrates and annealed at different temperatures are measured and analyzed in order to study the effect of annealing on active layer light absorption. After thermal annealing of P3HT:PCBM absorber layer, 100 nm-thick aluminum is deposited on top of the absorber layer as a cathode using a NRC thermal evaporator. Aluminum with a purity of 99.9% is purchased from Kurt J. Lesker. The main fabrication procedures are schematically shown at Figure 1.7. As it shows, four individual cells can be formed at one substrate and each of them has a size of about 0.25 cm^2. The area of each cell is defined by the overlap between strips of ITO and Al.

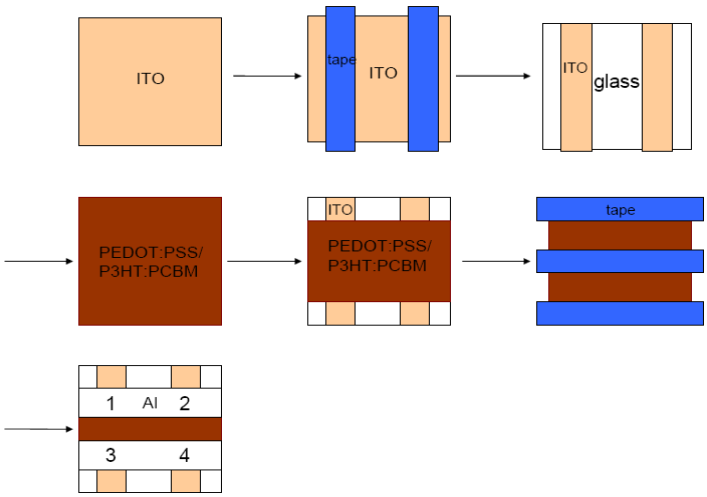

Figure 1.7: Fabrication procedures for polymer bulk heterojunction solar cell.

1.2.2 Characterization Tools

In this section, various characterization tools employed in this thesis work are introduced.

A profilometer (Figure 1.8(a)) is an instrument used to measure a feature's length or depth, usually in the micrometer or nanometer level. A stylus is moved vertically in contact with a sample and then moved laterally across the sample for a specified distance and specified contact force. It can measure small surface variations in vertical stylus displacement as a

function of position. This instrument has been used to measure thicknesses of the films. In this study, the KLA -Tencor Alpha-Step IQ Profilometer is used.

Ultraviolet-visible-near infrared (UV-VIS-NIR) spectroscopy is a useful technique for chemical and electronic band structure analysis by measuring the transmission (absorption) of light through (by) a sample. In this study, in order to investigate the light absorption of P3HT: PCBM active layer, Perkin Elmer Lambda 19 UV-VIS-NIR spectrometer (Figure 1.8(b)) is used.

The performance of the polymer photovoltaic cells fabricated is characterized using a home-made solar simulator (Figure 1.8(c)). The current versus voltage measurement is carried out under air mass (AM)0 condition using a Keithley 2420 3A source measurement unit controlled by a computer program written by NASA Glenn Research Center. Projector lamp (GE lighting General) is used to simulate AM0 and the crystalline silicon solar cell calibrated for AM0 at NASA Glenn Research Center is used to calibrate the projector lamp.

(a) (b) (c)

Figure 1.8: (a) KLA -Tencor Alpha-Step IQ Profilometer, (b) Perkin Elmer Lambda 19 UV-VIS-NIR spectrometer and (c) Home-made solar simulator.

1.3 Results and Discussion

1.3.1 Effect of the composition

It is observed that the change in PCBM content of the active layer greatly affects the cell performance. From Figures 1.9(a) and (c), it is found that J_{sc} and FF increase with the weight percentage of PCBM and reach the highest values of 1.32 mA/cm^2 and 21.7%

respectively when the PCBM weight percentage is 60 %. With the PCBM content increased further, both J_{sc} and FF go down.

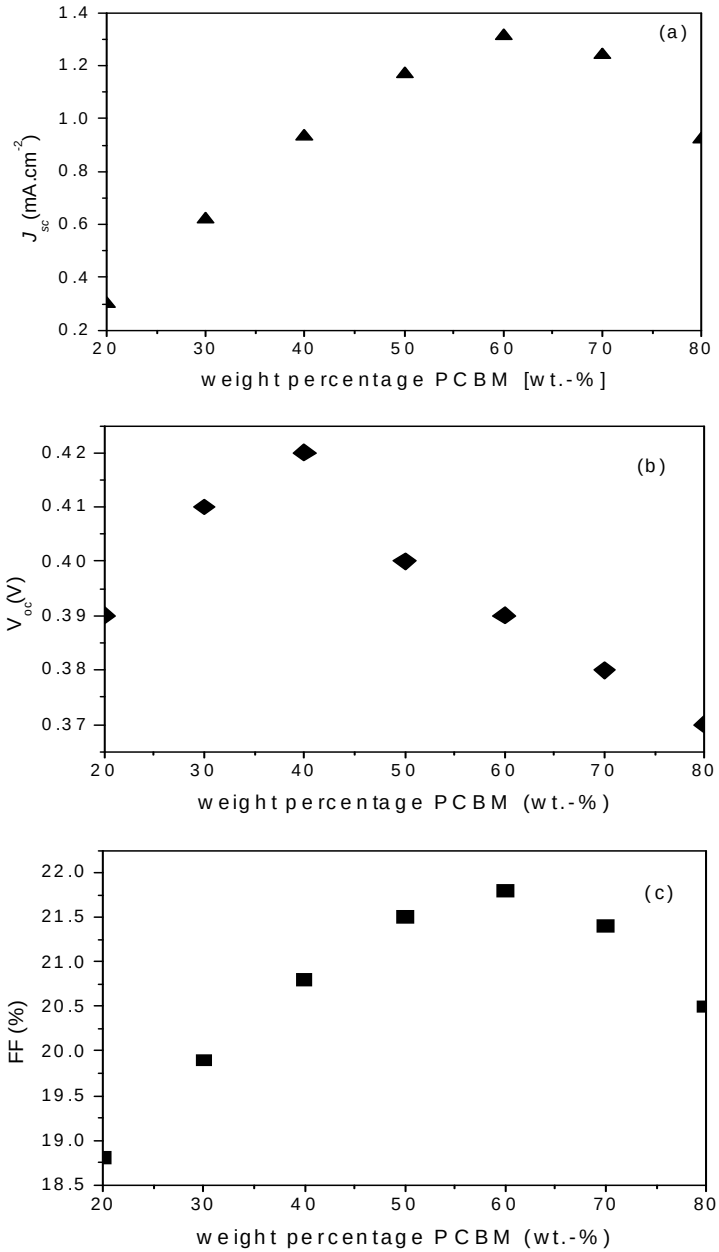

Figure 1.9: Performance of P3HT:PCBM bulk heterojunction solar cells as a function of weight percentage of PCBM; (a) short circuit current, (b) open circuit voltage, and (c) fill factor.

To achieve high J_{sc} and FF for polymer bulk heterojunction solar cells, creation of mobile charge carriers is important. As introduced, the mobile charge carriers can only be

generated at the P3HT/PCBM interfaces. Therefore too low of the PCBM content does not enable the required density of donor/acceptor interfaces. Additionally, too low of the PCBM concentration does not enable the required formation of the percolated electron transport paths. These two reasons can account for the J_{sc} and FF increase with PCBM concentrations from 20% to 60% according to Figure 1.9(a) and (c). However, it has been proved that PCBM tends form clusters, i.e. many PCBM molecules gather together, by molecular diffusion when it goes up to certain concentration [20]. This inhomogeneous distribution of PCBM within the P3HT matrix can decrease both the density of donor/acceptor interfaces and percolated electron transport paths, which is responsible for the decease of J_{sc} and FF when the PCBM concentration is over 60% in this study.

When it goes to V_{oc} (Figure 1.9(b)), it is found that V_{oc} increases with the PCBM percentage and reach the highest value of 0.43 V when the PCBM weight percentage is 40 %. With the PCBM content increased further, V_{oc} starts going down. This variation of V_{oc} can be explained by the shunt resistance (R_s) change with different PCBM percentage. When the PCBM percentage is low, P3HT phase is dominant so that there may exist shunts caused by the direct contact of P3HT with ITO and Al, because there is no enough PCBM phase to form charge separation interfaces. When the PCBM percentage is too high, the dominant PCBM phase may also generate shunts. In both conditions, the shunt resistance will decrease and result in a decrease of V_{oc}.

Therefore in this study, the influences of J_{sc} and FF on cell performance are determinant and the optimum PCBM weight percentage is found to be 60%.

1.3.2 Effect of solution concentration

The thickness of P3HT:PCBM active layer formed by spin coating can be determined by the solution concentration. In this study, the PCBM weight percentage is fixed to 60% according to the conclusion from previous study and the solution concentrations are varied. From Figures 1.10(a) and (c), it is found that both J_{sc} and FF increase with the solution concentration and

reach the highest value of 2.0 mA/cm^2 and 21.6% respectively when the total concentration is 36 mg/ml. With further increase in the solution concentration, both J_{sc} and FF go down.

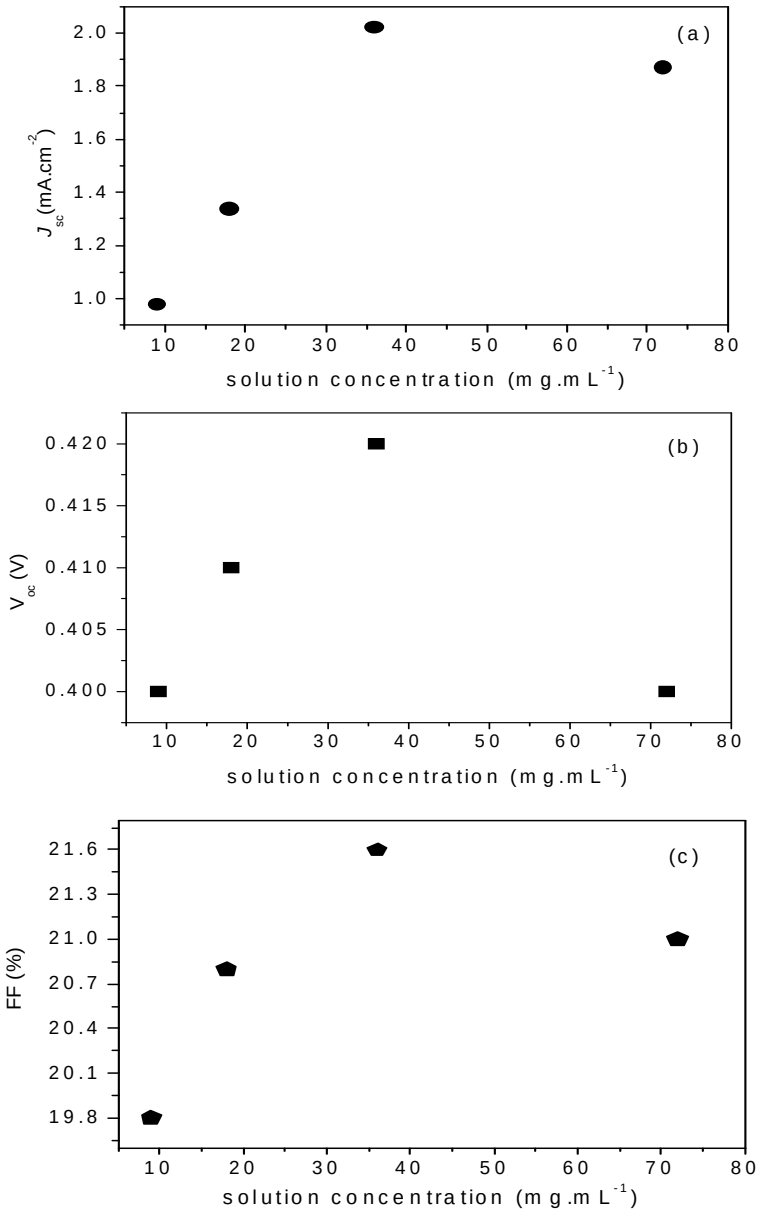

Figure 1.10: Performance of P3HT:PCBM bulk heterojunction solar cells as a function of solution concentration; (a) short circuit current, (b) open circuit voltage, and (c) fill factor.

The influence of solution concentration on J_{sc} and FF can be explained by the active layer thickness. With the increase of solution concentration, i.e. the increase of active layer

thickness, more excitons are generated due to the enhancement of light absorption. However, the resistance of the active layer also increases with thickness. Too high thickness will lead to the decrease of J_{sc} and FF. Therefore, the balance between active layer light absorption and resistance can be responsible for what is observed in this study.

When it goes to V_{oc} (Figure 1.10(b)), it is found that V_{oc} increases with the solution concentration and reaches the highest value of 0.42 V when the total concentration is 36 mg/ml, the same as J_{sc} and FF. It can be explained by the enhancement of light absorption. With further increase in the solution concentration, it starts to go down.

The decrease of V_{oc} can be explained by the solubility of P3HT and PCBM in chlorobenzene. When the solution concentration reaches 72 mg/ml, P3HT and PCBM may not be able to be dissolved completely but exist in the solution as particles. These particles can remain on the active layer after spin-coating and act as shunts which result in the decrease of V_{oc}.

1.3.3 Effect of Annealing

A set of three devices is fabricated under different annealing conditions. While the cell #D1 is not annealed after the blend of P3HT:PCBM was spin-coated on the PEDOT:PSS layer, the P3HT:PCBM blends in the cells #D2 and #D3 are annealed respectively at 80 ℃ and 150 ℃ for 20 minutes prior to the deposition of the cathode. The *I-V* characteristics and the solar cell output characteristics are shown in Figure 1.11 and Table 1.

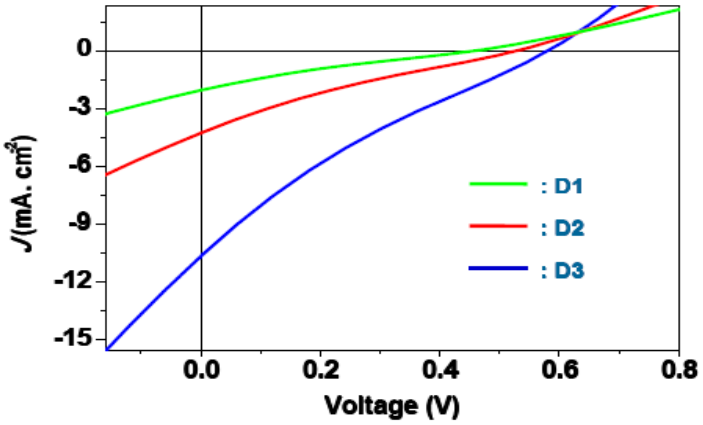

Figure 1.11: *I-V* characteristics of P3HT:PCBM bulk heterojunction solar cells as a function of annealing temperature.

Table 1.1: Solar cell output characteristics P3HT:PCBM bulk heterojunction solar cells as a function of annealing temperature.

Device no	J_{sc} (mA·cm⁻²)	V_{oc} (V)	FF (%)	PCE (%)
D1	2.04	0.47	21	0.20
D2	5.01	0.53	21	0.56
D3	10.65	0.58	22	1.36

According to Figure 1.11 and Table 1.1, it is concluded that both J_{sc} and V_{oc} of the cells increase with the increase of annealing temperature. D3 shows an efficiency of 1.36 %, more than two times higher than that of D1, which is only 0.20 %.

The observed increase in J_{sc} can be explained by phase separation of P3HT and PCBM by annealing. In order to achieve high efficiency solar cells, charge separation and the transport of the carriers to the electrodes, i.e. the continuous path ways for each carrier type, are very important and highly dependent on active layer morphology. It has been known that the annealing temperature should be higher than the glass transition temperature (T_g) of the polymer to realize crystallization because the mobility needed for crystallization is frozen below its T_g [21]. According to Zhao *et al* [22], T_gs for pure P3HT and PCBM are 12.1 ℃ and 131.2 ℃ respectively. According to the phase diagram (non-equilibrium) of P3HT/PCBM blends reported

in their work (Figure 1.12), T_g varies as a function of the composition of the blend. Since the weight percentage of PCBM is 60% in this study, the T_g for the blends is around 50 ℃. Consequently, annealing procedures need at least a temperature of 50 ℃ to realize the phase separation. In this study, it is confirmed by the cell performance improvement when annealed above 50 ℃.

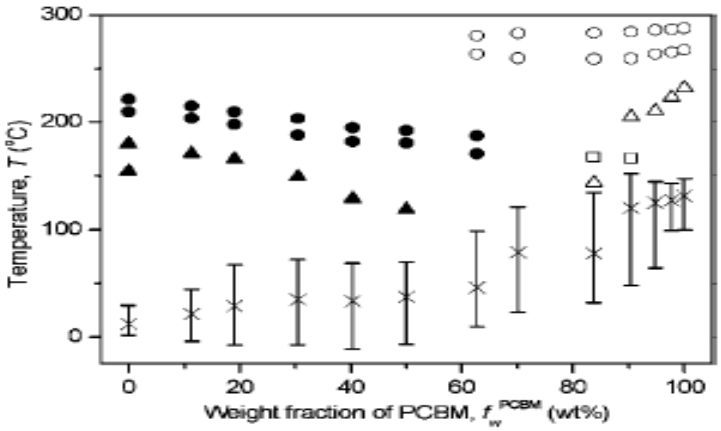

Figure 1.12: Phase diagram of P3HT/PCBM blends: melt crystallization temperature (▲) and melting temperature (●) of P3HT; melt crystallization temperature (Δ), cold crystallization temperature (□), and melting temperature (○) of PCBM; and Tg(x) with its range (vertical bar) of the blends [22].

In the case of P3HT, which has one molecular axis much longer than the other two, large p-conjugation length along the long axis and close molecular packing of the molecules along at least one of the short molecular axes are two important conditions for high carrier mobility [23]. These two conditions can be realized by P3HT crystallization upon annealing. Therefore higher carrier mobility caused by annealing is also responsible for the increase of J_{sc}.

According to what is discussed above, cell performance should increase as long as the device is annealed above 50 ℃, i.e. the T_g of P3HT. However, from Figure 1.11, it is also observed that the cell annealed at 150 ℃ shows the highest efficiency. Annealing at a higher temperature can promote the crystallization of P3HT creating a better donor/accepter phase separation and providing a higher carrier mobility.

One more interesting observation made during annealing is that the color of the active layer becomes darker. This clue gives the speculation that there may be an optical property change for active layer by annealing. To confirm this, a set of three P3HT:PCBM thin films arespin-coated on top of quartz substrates and UV-VIS-NIR spectroscopy is performed to measure their transmittance. While S1 indicates P3HT:PCBM layer without annealing, S2 and S3 are P3HT:PCBM blends annealed at 80 ℃ and 150 ° C respectively for 20 minutes (Figure 1.13). According to the figure, S2 and S3 show a lower transmittance than that of S1. It proves that by annealing, light absorption of P3HT:PCBM thin film is increased. The apparent modification of the P3HT:PCBM absorption spectrum can be attributed to a result of π-π overlap between main chains increases when the devices are annealed, resulting in a redshift of the P3HT absorption maximum as observed [24].

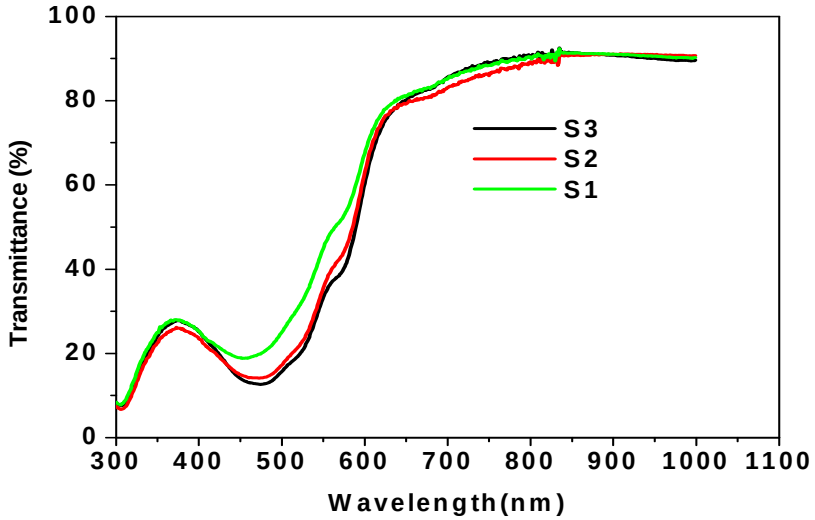

Figure1.13: UV–VIS-NIR spectra of the P3HT:PCBM blends annealed at various conditions; S1 – without annealing, S2 – 80 °C for 20 min, and S3 – 150 °C for 20 min.

The increase of V_{oc} with annealing temperature can be attributed to the shift of P3HT and PCBM band structures. It is known that for P3HT/PCBM solar cell, V_{oc} is mainly determined by the energy difference between the HOMO of P3HT (electron-donor) and the LUMO of PCBM (electron-acceptor). Due to the rearrangement of P3HT molecular chains by annealing, the π-π

overlap between main chains changes. It results in the change of HOMO and LUMO for P3HT and thus the various values of $V_{oc.}$

1.4 Conclusion

It is concluded that the efficiency of polymer bulk heterojunction solar cell is highly dependent on the preparation condition of the active layer and its consequent morphology. Various batches of the devices have been prepared to study the influences of P3HT:PCBM blend composition, solution concentration, and the thermal annealing on the cell performance. 60 wt% of PCBM in the blend is found to be the optimum composition under which both high density of donor and accepter interfaces and the formation of efficient percolated electron transport paths can be expected, leading to a high J_{sc} and FF. The optimum solution concentration of P3HT:PCBM blend has been found to be 36 mg/ml and it can be explained by the relationship between the active layer thickness and resistance. Finally, by thermal annealing, it is observed that the J_{sc} and V_{oc} increase from 2.04 mA and 0.47 V to 10.65 mA and 0.58 V respectively. The increase in J_{sc}, in particular, can be explained in terms of donor/accepter phase separation and charge carrier mobility increase caused by P3HT crystallization. The light absorption increase in active layer by annealing is also one reason why the J_{sc} increases. However, in this work, the FF, an important factor determining efficiency, cannot be increased by the morphology control of the active layer. Chapter 2 will focus on improving FF using a calcium/aluminum bilayer cathode.

CHAPTER 2

REALIZATION OF EFFICIENT ORGANIC SOLAR CELL WITH CALCIUM/ALUMINUM CATHODE

This chapter of the thesis describes the addition of Ca as a part of cathode into the device structure explained in chapter 1 and how device performance can be affected. Different metal/semiconductor interfaces and their influences on device performance are described first. Next the experimental procedures and the results for P3HT:PCBM bulk heterojunction solar cell with Ca/Al cathode are given.

2.1 Introduction

The metallic electrodes in optoelectronic devices are vital components because charge collection and injection at the electrodes closely depend on their electronic properties with respect to the part of the device it is interfacing with. An ideal electrode must be highly conductive, chemically and electrochemically stable and should not cause the degradation of the active materials contacted in the device [25, 26].

When a metal is considered as electrode material, its work function with respect to its interfacing material in the device configuration is critical because it will determine the function of the interface – either facilitate or hamper the flowing of charge carriers from the semiconductor to the contacts [27, 28].

At the contact between two different materials, there is equalization of the chemical potential of the electron, i.e. of the Fermi level, in the two different materials. At the contact between a metal and a semiconductor, either a rectifying Schottky or an ohmic contact is achieved [29].

If Φ_M is the work function of the metal and Φ_S is the work function of the semiconductor, there will be following cases:

- For n-type semiconductor

• a Schottky contact if $\Phi_M > \Phi_S$; electrons diffuse from the semiconductor to the metal and the depletion layer appears in the semiconductor. Consequent rectifying contact is shown in Figure 2.1.

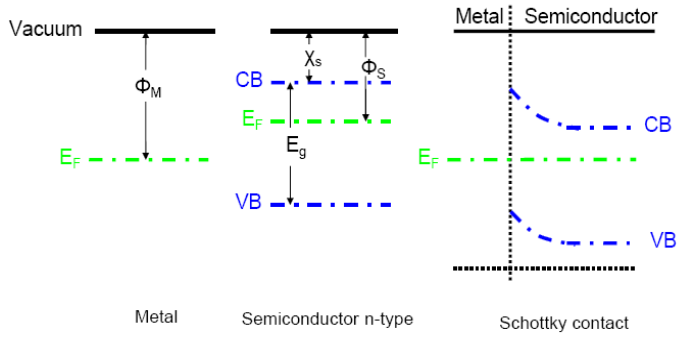

Figure 2.1: Schottky junction between a metal and n-type semiconductor with $\Phi_M > \Phi_S$.

• an ohmic contact if $\Phi_M < \Phi_S$; electrons diffuse from the metal to the semiconductor, and it creates a negative accumulation in the n-type semiconductor. Consequent ohmic junction without a barrier is shown in Figure 2.2.

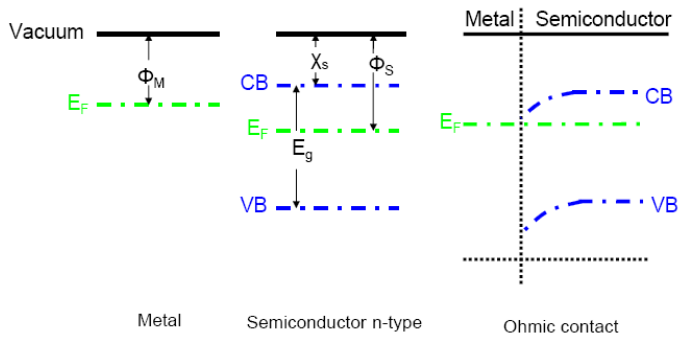

Figure 2.2: Ohmic junction between a metal and n-type semiconductor with $\Phi_M < \Phi_S$.

- For p-type semiconductor

• a Schottky contact if $\Phi_M < \Phi_S$; holes diffuse from the semiconductor to the metal and a depletion layer appears in the semiconductor. Consequent rectifying junction is shown in Figure 2.3.

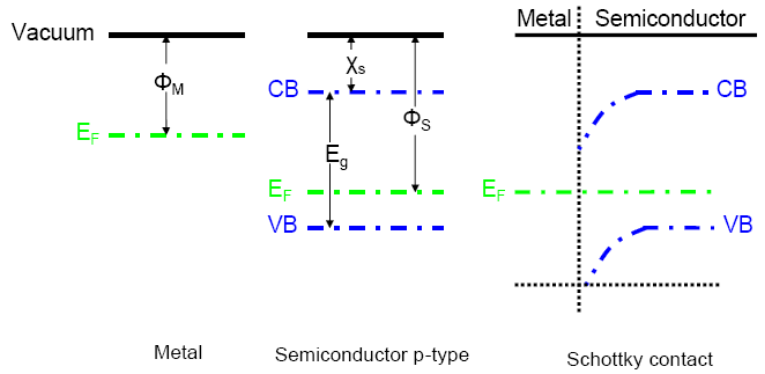

Figure 2.3: Schottky junction between a metal and p-type semiconductor with $\Phi_M < \Phi_S$.

• an ohmic contact if $\Phi_M > \Phi_S$; electrons diffuse from the semiconductor to the metal and it creates a positive accumulation in the p-type semiconductor. Consequent ohmic junction without a barrier is shown in Figure 2.4 [30].

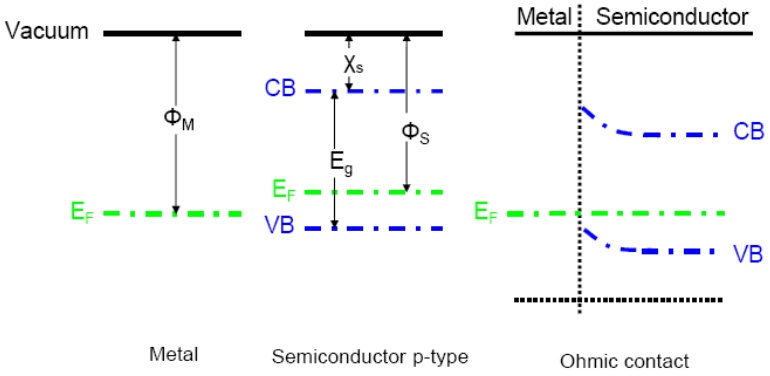

Figure 2.4: Ohmic junction between a metal and p-type semiconductor with $\Phi_M > \Phi_S$.

2.2 Electrode Materials for Polymer Solar Cells

For P3HT/PCBM bulk heterojunction solar cells, ITO is widely used because of its high transparency and good conductivity [31]. Also ITO has a high work function value of 4.7 eV, which makes it a good anode material to form ohmic junction with organic semiconductors [32]. As it shows in Figure 2.5, when ITO interfaces PEDOT:PSS (hole transport layer), there is no energy barrier at the interface because PEDOT:PSS has the same work function value of 4.7 eV as ITO [33].

For cathode that interfaces PCBM (electron acceptor), Al is normally used because of its good conductivity and stability in air [34]. Also the work function of aluminum (Φ_{Al}) is 4.3 eV, lower than that of PCBM (Φ_{PCBM} = 4.4 eV) and theoretically an ohmic junction can be formed at the interface [35]. This can explain the high efficient polymer bulk heterojunction solar cells using Al as cathode reported from the literature [36].

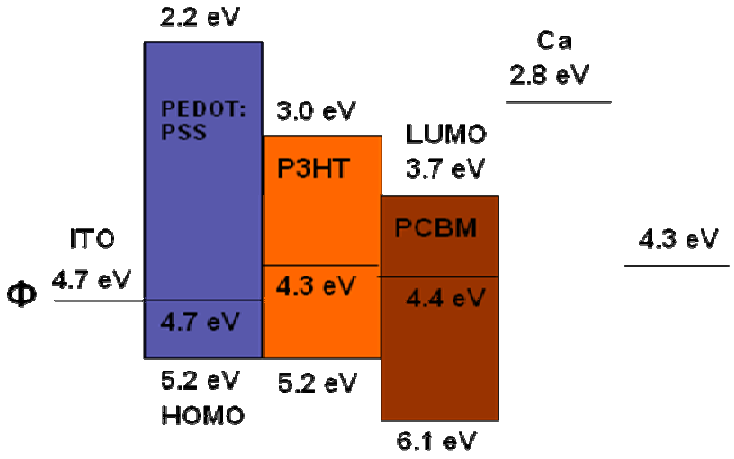

Figure 2.5: Energy diagram for device components [33-36].

2.3 Fill Factor in Polymer Solar Cells

FF is a more sensitive parameter compared to V_{oc} and J_{sc}, and depends on the mobility (m) – lifetime (t) product of the bulk material, thickness of the active polymer layer and the morphology of the cathode/polymer interface [37]. Dhritiman Gupta *et al.* confirmed that a nonuniform contact can result in a scenario of charge accumulation leading to a barrier formation at the cathode/polymer interface [38]. During thermal evaporation, the homogeneity of Al cathode layer is sensitive to the experimental conditions, such as sample placement, deposition rate and chamber pressure. Therefore it is speculated that the low FF observed in previous study may result from the inhomogeneous contact of Al cathode to the absorber layer.

Different deposition conditions (sample placement, deposition rate and chamber pressure) tried for Al in this study, however, have no effects on FF. Instead, the removal of charge accumulation was tried using a low workfunction metal – Ca - in the following study.

2.4 Ca/Al Bilayer Cathode for P3HT:PCBM Solar Cells

As introduced, when a metal and semiconductor with different work functions are placed in contact, electrons will flow from one with the lower work function until the Fermi levels equilibrate. The resulting electrostatic potential is termed the built-in field designated by V_{bi} and $V_{bi} = \Phi_s - \Phi_M$. The magnitude of V_{bi} determines how much it can hamper or facilitate the flowing of charge carriers to contact for Schottky or ohmic junction respectively and is expressed by the degree of band bending shown in the energy band diagram as described in earlier sections [39].

According to Figure 2.6, for both Al and Ca, the band bending facilitates the flowing of electrons to cathodes because of the formation of ohmic junctions. However, because the work function of Ca (Φ_{Ca}) is as low as 2.8 eV, the degree of band bending for Ca is higher ($V_{bi} = \Phi_{PCBM} - \Phi_{Ca} = 1.6$ eV) than that for Al ($V_{bi} = \Phi_{PCBM} - \Phi_{Al} = 0.1$ eV). Therefore using Ca, electrons can be transported to cathode more efficiently and it can help eliminate the charge accumulation. Al is deposited on top of Ca as a protection layer due to the poor stability of Ca in air.

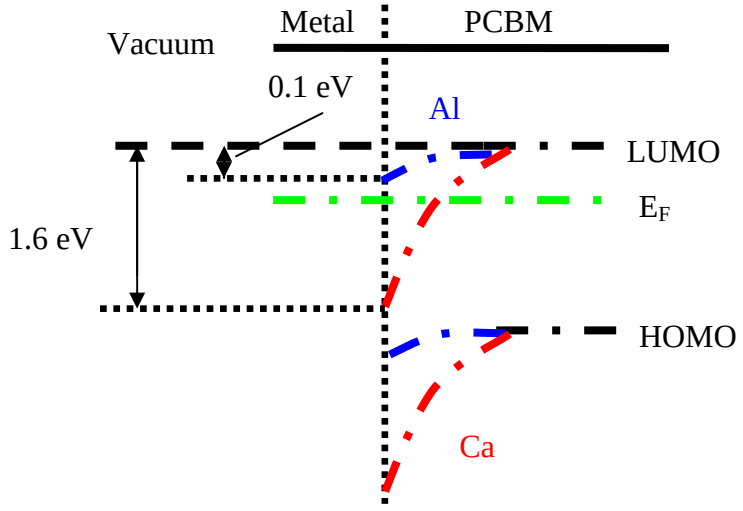

Figure 2.6: Energy band diagrams for Al (blue) and Ca (red) contacting with PCBM.

In this work, Ca/Al bilayer is used as the cathode and its influence on cell performance, especially on FF is studied.

2.5 Experimental Procedures

99.99% pure Ca and Al are purchased from Kurt J. Lesker for thermal evaporation. Because Ca is easily oxidized in the air, it is stored in the mineral oil and the oil is removed prior to the deposition. P3HT/PCBM solar cells respectively with only Al (D1) and Ca/Al (D2) are fabricated to compare the effects of Ca on cell performance. Thicknesses of Al and Ca are 100 nm and 50 nm respectively. The device measurements are carried out typically right after cathode deposition under AM0 condition using the solar simulator described in chapter 1.

2.6 Results and Discussions

According to Figure 2.7 and Table 2.1, it can be observed that FF increases from 21% to 51% by replacing Al with the Ca/Al cathode. Also, both J_{sc} and V_{oc} of the cells increase from 9.81 mA/cm^2 to 11.22 mA/cm^2 and 0.53 V to 0.65 V, respectively. An efficiency of 3.32% is realized for D2.

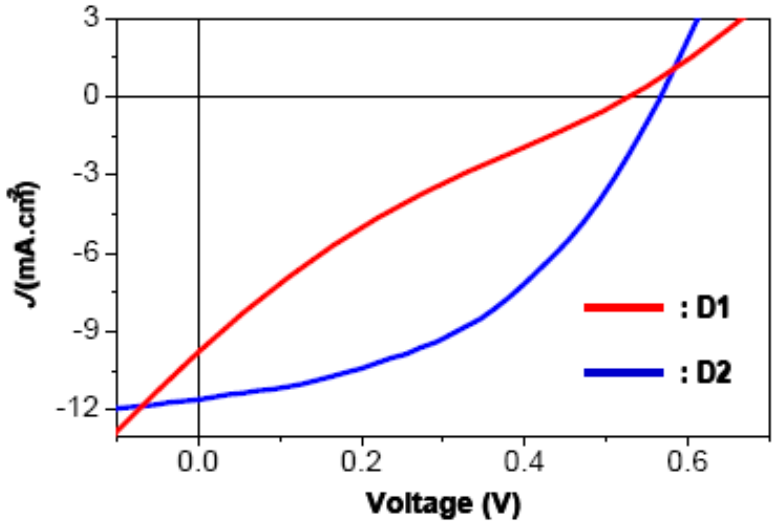

Figure 2.7: *I-V* characteristics of P3HT:PCBM solar cells with Al (D1) and Ca/Al bilayer (D2) as cathodes.

Table 2.1: Performance of P3HT:PCBM solar cells with Al (D1) and Ca/Al bilayer (D2) as cathodes.

Device no.	J_{sc} ($mA \cdot cm^{-2}$)	V_{oc} (V)	FF (%)	PCE (%)
D1	9.81	0.53	21	1.10
D2	11.22	0.58	51	3.32

The increase of J_{sc} and FF can derive from a removal of energy barrier caused by charge accumulation at the metal/PCBM by the addition of Ca. The increase of V_{oc} can be attributed to the higher work function difference between anode and cathode when Ca is added. As discussed in Chapter 1, V_{oc} is controlled primarily by the energy difference between the HOMO of P3HT (electron-donor) and the LUMO of PCBM (electron-acceptor). However, it is also dependent on the electric field generated by the work function difference between anode and cathode, although not as much as other polymer diodes with a metal-intrinsic-metal (MIM) structure [40]. Due to the lower work function of Ca than that of Al, a higher electric field enhances the $V_{oc.}$

2.7 Conclusion

P3HT/PCBM polymer bulk heterojunction solar cells with Ca/Al cathode are fabricated to study the effect of Ca on the cell performance. Compared to cells with Al cathode, FF of the cells with Ca/Al cathode has increased from 21% to 51%. Also the increases of J_{sc} and V_{oc} are observed. The improvement can be attributed to the removal of charge accumulation at the metal/PCBM interface caused by the high V_{bi} when the low work function Ca is used.

REFERENCES

[1] C. J. Brabec, J. A. Hauch, P. Schilinsky, and C. Waldauf, *MRS Bulletin.* **30**, 50 (2005).

[2] http://en.wikipedia.org/wiki/Photovoltaic

[3] http://blog.disorderedmatter.eu

[4] Y. B. Yoon, T. W. Kim, H. W. Yang, J. H. Kim, J. H. Seo, and Y. K. Kim, *Thin solid Films* **515**, 5095 (2007).

[5] R. A. J. Janssen, J. C. Hummelen, and N. S. Sariciftci, *MRS Bulletin.* **30**, 335 (2005).

[6] G. Yu, J. Gao, J. C. Hummelen, F. Wudl, and A. J. Heeger, *Science* **270**, 1789 (1995).

[7] J. J. M. Halls, C. A. Walsh, N. C. Greenham, E. A. Marseglia, R. H. Friend, S. C. Moratti, and A.B. Holmes, *Nature* **376**, 498 (1995).

[8] L. Gang, V. Shrotriya, J. Huang, Y. Yao, T. Moriarty, K. Emery, and Y. Yang, *Nature Materials* **4**, 865 (2005).

[9] W. L. Ma, C. Y. Yang, X. Gong, K. Lee, and A. J. Heeger, *Adv. Funct. Mater.* **15**, 1622 (2005).

[10] G. Li, V. Shrotriya, J. S. Huang, Y. Yao, T. Moriarty, K. Emery, and Y. Yang, *Nat. Mater.* **4**, 864 (2005).

[11] H. Hoppe, and N. S. Sariciftci, *J. Mater. Chem*. **16**, 47 (2006).

[12] S. E. Shaheen, C. J. Brabec, N. S. Sariciftci, F. Padinger, T. Fromherz and, J. C. Hummelen, *Appl. Phys. Lett.* **78**, 841 (2001).

[13] J. Gao, F. Hide, and H. Wang, *Synth. Met*. **84,** 979 (1997).

[14] A. M. Nardes, PhD Thesis, the Eindhoven University of Technology (Netherlands) (2007).

[15] A. Ashok, Thesis, Electrical Characterization of conjugated polymer light emitting devices (2004).

[16] J. Zhang, A. L. Barker, D. Mandler, and P. R. Unwin, *J. Am. Chem. Soc*. **125**, 9312 (2003).

[17] T.A. Chen, and R. Rieke, *J. Am. Chem. Soc.* **114**, 10087 (1992).

[18] http://www.nano-c.com/fullerenederivatives.html

[19] G. Janssen, A. Aguirre, E. Goovaerts, P. Vanlaeke, J. Poortmans, and J. Manca, *Eur. Phys. J. Appl. Phys*. **37**, 287 (2007).

[20] D. Chirvase, J. Parisi, J. C. Hummelen, and V. Dyakonov, *Nanotechnology* **15**, 1320 (2004).

[21] J. Zhao, A. Swinnen, G. V. Assche, J. Manca, D. Vanderzande, and B. V. Mele, *J. Phys. Chem.* **113***,* 1589 (2009).

[22] F. Padinger, R. S. Rittberger, and N. S. Sariciftci, *Adv. Funct. Mater.* **13,** 1 (2003)

[23] C. D. Dimitrakopoulos, and D. J. Mascaro, *IBM J. RES. & DEV.* **45**, 18 (2001).

[24] C. Yang, F. P. Orfino, and S. Holdcroft, *Macromolecules* **29**, 6510 (1996).

[25] H. Spanggaard, and F. C. Krebs, *Solar Energy Materials and Solar Cells* **83**, 128 (2004).

[26] R. O. Loutfy, J. H. Sharp, C. K. Hsiao, and R. Ho, *Journal of Applied Physics* **52**, 5220 (1981).

[27] A. K. Ghosh, D. L. Morel, T. Feng, R. F. Shaw, and C. A. Rowe, *Journal of Applied Physics* **45**, 235 (1974).

[28] G. D. Sharma, S. K. Gupta, and M. S. Roy, *Journal of Physics and Chemistry of Solids* **58**,198 (1997).

[29] S. M. Sze, *Physics of semiconductor devices*, 2nd Edition, John Wiley & Sons, New York, 1981.

[30] H. Mathieu, *Physique des semiconducteurs et des composants électroniques*, 2nd Edition, Masson, Paris, 1990.

[31] http://en.wikipedia.org/wiki/Indium_tin_oxide

[32] L. Chkoda, C. Heske, M. Sokolowski, E. Umbach, F. Steuber, J. Staudigel, and J.

Simmerer, *Synthetic Metals* **111**, 317 (2000).

[33] A. M. Nardes, M. Kemerink, M. M. de Kok, E. Vinken, K. Maturova, and R. A. J. Janssen, *Organic Electronics* **9,** 729 (2008).

[34] http://en.wikipedia.org/wiki/Aluminium

[35] H. Hoppe, T. Glatzel, M. Niggemann, W. Schwinger, F. Schaeffler, A. Hinsch, M. Ch. Lux-Steiner, and N. S. Sariciftci, *Thin Solid Films* **511**, 590 (2006).

[36] J. Y. Kim, S. H. Kim, H. H. Lee, K. Lee, W. Ma, X. Gong, and A. J. Heeger, *Adv. Mater.* **18**, 574 (2006).

[37] D. Gupta, M. Bag, and K. S. Narayan, *Appl. Phys. Lett.* **92**, 093301 (2008)

[38] D. J. Roulston, *An introduction to the physics of semiconductor devices*. Oxford University Press, New York, 1999.

[39] J. Xue, B. P. Rand, and S. R. Forrest, *Organic Photovoltaics VII* **6334**, 63340K (2006).

[40] V. D. Mihailetchi, P. W. M. Blom, J. C. Hummelen, and Rispens, *Journal of Applied Physics* **94**, 6852 (2003).

BIOGRAPHICAL INFORMATION

Yi Yang was born in Changzhi, China. He completed his Bachelor of Science in Light Chemical Engineering from Hebei University of Science and Technology, Shijiazhuang, China.

In fall 2007, he joined Materials Science and Engineering of the University of Texas at Arlington as a graduate student to obtain Master's Degree. He worked as a graduate research assistant in the Photovoltaics Materials Laboratory for two years. After completion of Master's degree, he will look for an engineer position in a solar cell company.